Balancing downlink and uplink soft-handover areas in UMTS networks

Lucas Benedičič and Mitja Štular
Telekom Slovenije, d.d.
Cigaletova 15, SI-1000, Ljubljana, Slovenia
Email: lucas.benedicic@telekom.si,
mitja.stular@telekom.si

Peter Korošec
Computer Systems Department,
Jožef Stefan Institute,
Jamova cesta 39, SI-1000, Ljubljana, Slovenia
Email: peter.korosec@ijs.si

***Abstract*—In this paper a static network simulator is used to find downlink and uplink SHO areas. By introducing a penalty-based objective function and some hard constraints, we formally define the problem of balancing SHO areas in UMTS networks. The state-of-the-art mathematical model used and the penalty scores of the objective function are set according to the configuration and layout of a real mobile network, deployed in Slovenia by Telekom Slovenije, d.d.. The balancing problem is then tackled by three optimization algorithms, each of them belonging to a different category of metaheuristics. We report and analyze the optimization results, as well as the performance of each of the optimization algorithms used.**

I. Introduction and motivation

In mobile networks, handover is one of the main features that allows user's mobility [9]. The concept behind the handover operation is simple: when a user moves from the coverage area of a cell to the coverage area of a neighboring cell, the system creates a new connection with latter cell and disconnects the user from the former one, while keeping the current connection active. Soft-handover (SHO), on the other hand, is a possibility available in mobile networks using the Wideband Code Division Multiple Access (WCDMA) technology, which the Universal Mobile Telecommunications System (UMTS) employs. SHO enhances handover functionality by allowing a user to potentially operate on multiple radio links in parallel. Since different users are separated by unique spreading codes, the detection of single user's signal is implemented by despreading with the same code sequence used in the transmitter [9].

Every mobile terminal constantly monitors the common pilot power channel (CPICH) of the connected cell and its neighbors. The information about these measurements is sent to the network by the user terminal (i.e. mobile). The SHO condition depends on the relative received signal quality from different cells and the SHO window, which triggers the addition of a cell to the user's active set. Depending on radio propagation characteristics and different transceiver capabilities, the radio transmission can gain more than 3 dB out of an SHO situation [9]. From this point of view, SHO is a method to reduce interference and improve radio quality, particularly at the cell border where radio coverage is of inferior quality. In UMTS Release 99 [22], SHO is specified to work from the network towards the user (i.e. downlink), and from the user towards the network (i.e. uplink).

With the introduction of High Speed Packet Access (HSPA) as an improvement of the performance existing in WCDMA protocols, the role SHO plays in mobile network configuration and functioning slightly changed. The key difference is that High Speed Downlink Packet Access (HSDPA) does not support SHO, while the High Speed Uplink Packet Access (HSUPA) does [10]. This particular distinction has some key implications in the balanced distribution of SHO areas, and thus in the achievable throughput of the HSPA services. Namely, deviations between downlink and uplink SHO areas create potential power control imperfections, which imply that the uplink connection requires a relatively high transmit power when the user is in SHO mode, since the uplink carries the acknowledge/not acknowledge messages and the link quality report [10]. Moreover, the power control from non-serving HSDPA cells may reduce the received power level in the SHO region, and therefore the connection throughput, as the user terminal has to reduce the uplink transmission power level if any of the neighboring cells sends a power-down command [10]. Also, since SHO gain is only available in the uplink direction during HSPA, the signals from neighboring cells appear as noise in the downlink.

The situations described above are expected during the normal functioning of a UMTS network with HSPA services. There are a number of built-in mechanisms that allow the network to continue working despite their presence [10]. These same mechanisms also help reducing the consequences of unbalanced SHO areas between downlink and uplink. Clearly, this comes at the price of sacrificing some quality of service, better understood as throughput in the context of HSPA.

However, some abnormal cases do arise because of the combined effect of these situations, especially where there is SHO capability in the uplink, but none in the downlink. An example of such a case is depicted in Figure 1, which shows interference behavior during a HSPA connection in normal SHO conditions (a), and in unbalanced SHO conditions (b). Graph data are actual radio network statistics, taken from the mobile network deployed in Slovenia by Telekom Slovenije, d.d.. The graph on the left (a) shows a normal HSDPA-enabled service situation, in which the measured interference is directly

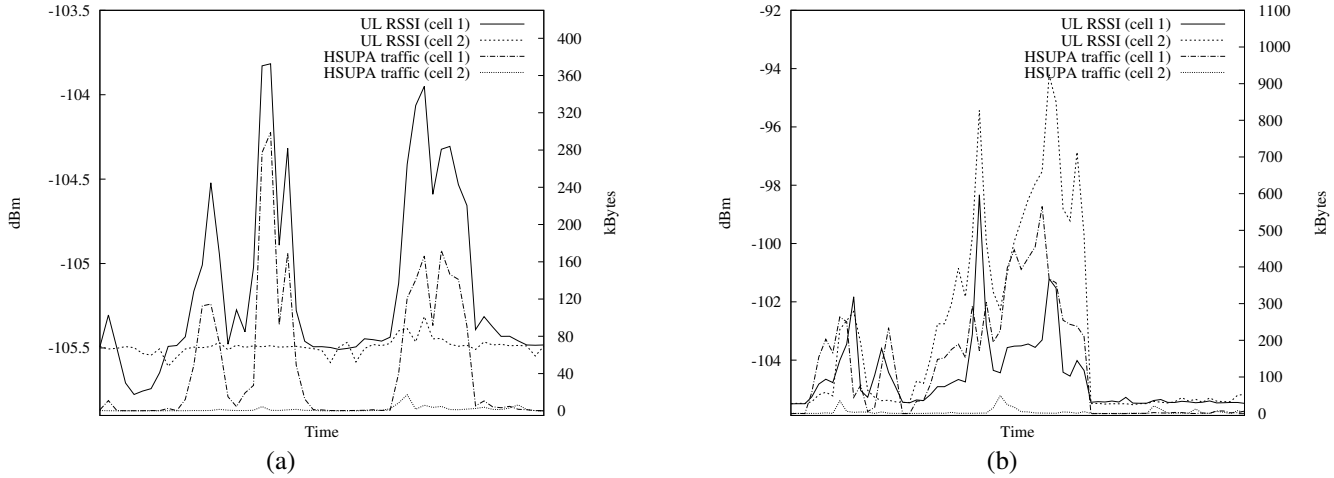

Figure 1. HSUPA traffic and uplink interference with: (a) balanced downlink and uplink SHO conditions; (b) unbalanced downlink and uplink SHO conditions.

proportional to the traffic being served. Note how the noise rises with the increased traffic on cell 1, while its neighbor (cell 2) has almost no interference nor traffic. Moreover, the graph profile for both traffic and noise of cell 1 are almost identical. The graph on the right (b) depicts a problematic situation, where the noise level does not only rise on the cell serving the HSDPA services (cell 1), but also on the neighboring one. Notice how the interference level rises on the cell that has almost no traffic (cell 2). It is clear that the source of this noise rise is generated on cell 1, which shows an increase in HSDPA traffic. However, the noise level profile in the serving cell does not mirror the traffic profile, as it did in the normal situation (a). This is due to power control imperfections that appear in unbalanced SHO areas when serving HSPA data.

Given the described context, the challenge is to achieve the correct balance or distribution of downlink and uplink SHO areas within a working UMTS network. Therefore, the network has to be fine-tuned to achieve a better SHO-area balancing, and thus avoiding the appearance of problematic situations as shown in Figure 1. This clearly implies that the mobile network configuration should not be excessively altered, since other aspects of the network are working well before starting the optimization process. Hence, we have decided to define an optimization problem which objective is to find a CPICH power level configuration for all the cells in the working network, such that the balance of downlink and uplink SHO areas is improved and other network aspects are preserved. The optimization process takes into account different kinds of hardware (e.g. amplifiers, cables, and antennas), but only the CPICH powers of the cells are to be changed.

In this paper we utilize a static network simulator, based on a state-of-the-art mathematical model [15], to find downlink and uplink SHO areas. By introducing a penalty-based objective function and some hard constraints, we formally define the problem of balancing SHO areas in UMTS networks. The mathematical model and the penalty scores of the objective function are set according to the configuration and layout of a real mobile network, deployed in Slovenia by Telekom Slovenije, d.d.. The SHO considered settings are also taken from actual network configuration, still they were adapted to closely model interference and other dynamics present in the network. The balancing problem is then tackled by three optimization algorithms, each of them belonging to a different category of metaheuristics. The optimization results, as well as the performance of each of the optimization algorithms used, are afterwards analyzed.

The remainder of this paper is organized as follows: in Section II we give an overview of other works related to CPICH-power and SHO optimization in UMTS. The static network model is presented in Section III, where all the elements of the mathematical model and the objective function are defined. In Section IV we introduce and shortly describe the optimization algorithms used to tackle the balancing problem. The simulations, including their environment and parameter setup are described in Section V, followed by their results in Section VI. We conclude with Section VII by giving a conclusion and guides for future work.

II. Related work

SHO optimization has received quite some attention from the scientific community in the last years. This mainly relates to the importance it has within deployed networks that provide high speed services such as video telephony [1] and Internet access by means of HSPA [3].

Some authors tackle optimization problems at the planning stage of the network [6], [8], considering, among other variables, base station locations and hardware. The fact is that most mobile operators are unable to apply these contributions to a live network since the planning phase has long been concluded. Moreover, the great majority of the base stations have already been deployed and their hardware also installed. Therefore, from the mobile operator's point of view, mainly

parameter and software optimization are the tools available when it comes to improvement of the quality of service and troubleshooting the network in the short term.

Optimizing SHO by means of CPICH is an established way of enhancing network capacity when high speed services like HSDPA an HSUPA coexist with legacy technologies [2]. The CPICH transmit power is typically between 5% to 10% of the total downlink transmit power of the base station [13], but there is no standardized method to find a CPICH power setting. A number of existing approaches to resolve this issue exist in the related literature (see [9], [17], [23]). The most effective ones are those based on optimization methods, but they are not always easy to implement or fast enough [6], [7], [13], [14], [18]. Such a wide spectrum of proposed procedures is directly related to the diverse criteria taken into account when assigning the CPICH power of a cell. The fundamental reason behind this fact is that the CPICH power is a common factor of various optimization problems in UMTS networks.

To the best of our knowledge, there is no reference in the literature to a simulation-based approach to find active downlink and uplink SHO areas. Additionally, as far as we know, the SHO balancing problem as described in this paper has not yet been tackled by any formal optimization method.

III. Mobile network model

Following the representation of a static network model from [15], this section addresses the definitions of all the elements included in the mathematical model used for the simulations.

Our goal here is to analyze the state of the network in a given situation, e.g. a 'snapshot' at an arbitrary instance. A snapshot consists of a set of users (or mobiles) having individual properties, such as location, and equipment type. The static approach inherently ignores dynamic effects that influence the system, like fast power control [15].

The mathematical model links the SHO settings with CPICH power settings for each cell, the best-server pattern, and the network coverage.

A. Basic elements

We start by considering a UMTS network with a set of antenna installations (cells), N. A pixel grid of a given resolution represents the service area, A, within which there is a set of mobiles, M. We denote $L^{\downarrow}_{im}$ as the downlink attenuation factor between cell $i \in N$ and mobile $m \in M$. Similarly, we define $L^{\uparrow}_{mi}$ as the uplink attenuation factor between mobile m and cell i. The attenuation factor values are calculated by performing signal propagation predictions for every pair (i, m), $i \in N$, $m \in M$, using the commercial radio planning tool TEMS^{TM} CellPlanner [21]. These predictions already include losses and gains from cabling, hardware, and user equipment.

By introducing a change step of 0.01 dB and bounding the CPICH power of a cell i to ± 2 dB, relative to the CPICH power setting the cell had before optimization, we define a finite set of candidate CPICH power settings for cell i as $P_i = \{p_i^1, p_i^2, ..., p_i^K\}$. By limiting the possible CPICH power settings a cell i may have, we are delineating two important aspects of the problem. First, since we are optimizing a live network, we do not want the algorithms to create complete new configurations, but just to fine-tune existing ones. Second, the problem complexity is lowered, because the size of the search space is smaller.

B. Coverage

A mobile m within the area A is under network coverage if at least one cell i covers it. We define the downlink coverage by means of the received signal code power (RSCP) [9]. Following the current network settings, and including a margin for interference derived from HSDPA [10], the RSCP threshold is set to -115 dBm ($3.16227766 \cdot 10^{-12}$ mW). So, for any pair (i, m), $i \in N$, $m \in M$, the coverage of mobile m by cell i is defined as

$$cov_{im} = \begin{cases} 1 & if\ RSCP_{im} \geq -115\, dBm \\ 0 & otherwise \end{cases}. \qquad (1)$$

If m is covered by more than one cell, we refer to the cell with the highest RSCP as the best server, an we denote it as i^*.

C. SHO areas

To obtain a realistic outline of the areas where a mobile may potentially maintain connections to more than one cell, we use a static version of the active set [15]. Therefore, we introduce a SHO window, γ^{SHO}, and a maximum active set size, n^{MAX}. Both parameters are taken from the current configuration of the network. The cells to which a mobile $m \in M$ may maintain concurrent connections are part of the set

$$SHO^{\downarrow}_m = \left\{ i | L^{\downarrow}_{i^* m} p_{i^*} - L^{\downarrow}_{im} p_i \leq \gamma^{\mathrm{SHO}} \right\}, \qquad (2)$$

where $i \in N$, $L^{\downarrow}_{i^* m}$ is the downlink attenuation factor of the cell with the strongest signal (best server), and p_{i^*} is its CPICH power. Since the number of elements in $SHO^{\downarrow}_m$ is at most n^{MAX}, the weakest links are removed if there are more present. This method is well suited for configurations with no hysteresis, since dynamic effects are ignored in static models [15].

Additionally, in the uplink, we define the set of cells to which a mobile can potentially be in SHO as

$$SHO^{\uparrow}_m = \left\{ i | L^{\uparrow}_{mi} P^{\uparrow}_m \geq 3.16227766 \cdot 10^{-12} mW \right\}, \qquad (3)$$

where $i \in N$, $L^{\uparrow}_{mi}$ is the uplink attenuation factor from mobile m to cell i, and $P^{\uparrow}_m$ is the uplink transmit power of mobile m.

Because of the static nature of the model, we are neglecting mobility and interference by narrowing the SHO window to 2 dB [15].

D. Optimization objective

Using the elements defined in Section III-C, we have constructed an objective function in cooperation with a team of radio engineers of the Radio Network Department at Telekom Slovenije, d.d.. The objective function is constructed as a weighted sum, containing different costs that penalize the occurrence of specific SHO conditions in downlink and uplink, which may potentially cause the aforementioned malfunctioning, introduced in Section I.

A cost-based objective function is the most natural and straight-forward way of defining the optimization objective. Besides it is easily extendable to include other future circumstances and it also defines the mutual importance of the different situations taken into account at the optimization phase.

Hence, the definition of the objective function for the balancing problem is the minimization of the sum of penalty scores given as

$$\begin{aligned} \min F \quad = \quad & \sum_{i \in N} \sum_{m \in M} pf_{\mathrm{COV}}(1 - cov_{im}) \\ & + pf^{\uparrow}_{\mathrm{SHO}} sho^{\uparrow}_{im}(1 - sho^{\downarrow}_{im}) \\ & + pf^{\downarrow}_{\mathrm{SHO}} sho^{\downarrow}_{im}(1 - sho^{\uparrow}_{im}), \end{aligned} \tag{4}$$

where

$$sho^{\downarrow}_{im} = \begin{cases} 1 & i \in SHO^{\downarrow}_{m} \\ 0 & otherwise \end{cases}, \tag{5}$$

$$sho^{\uparrow}_{im} = \begin{cases} 1 & i \in SHO^{\uparrow}_{m} \\ 0 & otherwise \end{cases}, \tag{6}$$

and

- pf_{COV} represents the penalty factor for uncovered areas,
- $pf^{\uparrow}_{\mathrm{SHO}}$ represents the penalty factor for uplink SHO areas where SHO is not possible in the downlink, and
- $pf^{\downarrow}_{\mathrm{SHO}}$ represents the penalty factor for downlink SHO areas where SHO is not possible in the uplink.

IV. Optimization algorithms

We tackled the problem of balancing SHO areas using three fundamentally different optimization algorithms, namely:

- differential evolution, from the family of evolutionary algorithms;
- differential ant-stigmergy algorithm, from the family of swarm-intelligence algorithms; and
- simulated annealing, from the group of classic metaheuristic algorithms, targeted at combinatorial optimization problems.

A. Differential evolution

Differential evolution (DE) [19] is a simple and powerful evolutionary algorithm proposed for global optimization. A wide range of optimization problems have been solved by applying DE [4]. The algorithm exhibits a parallel direct search method, which utilizes D-dimensional parameter vectors. The balancing problem is expressed in each component of a vector X of the population, which maps to the CPICH power of one cell under optimization:

$$X_{aG} = \{x_1, x_2, \ldots x_i, \ldots, x_D\}, \tag{7}$$

where $x_i \in P_i$ represents a candidate CPICH power setting of cell i, and G indicates the generation of an individual a in the population. Since there are $|N|$ cells in the mobile network, it follows that $D = |N|$.

In each generation, DE produces new parameter vectors by adding the weighted difference between two population vectors to a third one [19]. The resulting vector is retained if it yields a lower objective function value than a predetermined population member; otherwise, the old vector is kept.

There are different variants of DE. We have chosen the most popular one to solve our optimization problem, called *DE/rand/1/bin*. The nomenclature used to name this variant indicates the way the algorithm works:

- *DE* denotes the differential evolution algorithm,
- *rand* indicates that the individuals selected to compute the mutation values are randomly chosen,
- 1 specifies the number of pairs of selected solutions used to calculate the weighted difference vector, and
- *bin* means that a binomial recombination operator is used.

We considered four parameters to control the search process of DE: the population size, the maximum number of generations for the algorithm to run, the crossover constant, and the mutation scaling factor.

An extensive description of DE and its variants may be found in [16].

B. Differential ant-stigmergy algorithm

Based on the metaheuristic Ant-Colony Optimization (ACO) [5], the differential ant-stigmergy algorithm (DASA) [12] provides a framework to successfully cope with high-dimensional numerical optimization problems. It creates a fine-grained discrete form of the search space, representing it as a graph. This graph is then used as the walking paths for the ants, which iteratively improve the temporary best solution.

The mapping between the balancing problem and DASA is similar to the one depicted in Equation (7):

$$X_a = \{x_1, x_2, \ldots x_i, \ldots, x_D\} \tag{8}$$

In this case, each ant, a, creates its own solution vector, X_a, during the minimization process. At the end of every iteration, and after all the ants have created solutions, they are evaluated to establish if any of them is better than the best solution found so far.

There are six parameters that control the way DASA explores the search space: the number of ants, the discrete base, the pheromone dispersion factor, the global scale-increasing factor, the global scale-decreasing factor, and the maximum parameter precision.

For a more in-depth explanation about these parameters and the DASA algorithm itself, we refer the reader to [12].

C. Simulated annealing

As the third optimization algorithm to tackle the balancing problem we have chosen simulated annealing (SA) [11], a classic metaheuristic algorithm often used when the search space is discrete. SA has proved to be a solid optimization algorithm, capable of giving high-quality solutions to a wide scope of optimization problems [20].

At each time step during the process, the system under optimization is in a given *state*. The objective function maps a system state to a value known as the *energy* of the system in that state. A *move* in the search space represents a change in the state of the system. After making a move, the system may exhibit lower or higher energy, depending on the results of the objective function. When dealing with minimization problems, a better state always describes lower energy than the previous one.

SA incorporates the notion of *temperature*, by which the probability of moving the current state of the system into a worst one is lowered as the temperature decreases. Exploration of the search space is thus induced at higher temperature, whereas exploitation appears at lower temperature, when only improving moves are accepted.

Table I shows the pseudo-code executed of a move in the search space of possible CPICH power settings, resulting in a new state of the system.

Table I
PSEUDO-CODE: A MOVE IN THE SEARCH SPACE OF SA.

Step	
1	$i' = random\,cell(N)$
	do
2	$if\, rand() < 0.5\, then\, p_{i'}^{\mathrm{NEW}} = p_{i'} + 0.01$
	$else\, p_{i'}^{\mathrm{NEW}} = p_{i'} - 0.01$
3	**while** $p_{i'}^{\mathrm{NEW}} \notin P_{i'}$
4	$p_{i'} = p_{i'}^{\mathrm{NEW}}$

At the first step, a cell, i', is randomly selected from the set of all cells in the network, N. In step 2, a change of +0.01 dB or -0.01 dB is applied with 50% probability to $p_{i'}$. The current CPICH power of cell i' is expressed in dBm. The randomly generated CPICH power setting, $p_{i'}^{\mathrm{NEW}}$, it's checked for validity in step 3, i.e. it must be an element of the set $P_{i'}$. If $p_{i'}^{\mathrm{NEW}}$ is not a valid CPICH power, step 2 is executed again, generating another random CPICH power. Finally, in step 4, the CPICH power of cell i is replaced by $p_{i'}^{\mathrm{NEW}}$.

It is important to note that, as long as $|P_{i'}| > 1$, the algorithm shown in Table I shall never be trapped in an endless loop. On the other hand, if $|P_{i'}| < 2$, there are no candidate CPICH powers for cell i' and thus no possibility of optimization by means of CPICH power adjustment.

Notice also that the acceptance of a move in the search space is left to SA and its stochastic components.

V. SIMULATIONS

The simulations are performed using a standard Monte-Carlo method, assuming the mobile users are uniformly distributed. The path-loss data were calculated in advance, using the commercial radio planning tool TEMS^{TM} CellPlanner [21]. The SHO conditions of different users depend on the relative received signal quality from different cells and the SHO window, which triggers the addition of a cell to the user's active set [9].

A. Test network

The test network used for the simulations is a subset of the real UMTS network deployed in Slovenia by Telekom Slovenije, d.d.. It represents a network extending over a hilly terrain, combining both rural and middle-dense suburban areas, which contains 25 cells within an area of more than 150 km^2. Table II shows some properties of the test network used.

Table II
TEST NETWORK PROPERTIES.

Number of cells	25
Coverage threshold (RSCP)	$-115\,dBm$
SHO window (γ^{SHO})	$2\,dB$
User equipment ($P_m^{\uparrow}$)	$21\,dBm$, power class 4
Pixel resolution	$25\,m^2$
Population density	$398/km^2$

B. Penalty factors

After extensive experimentation, and working in cooperation with the radio engineers from the Radio Network Department at Telekom Slovenije, d.d., the penalty factors from Equation (4) are set to the following values:

- $pf_{\mathrm{COV}} = 15$,
- $pf_{\mathrm{SHO}}^{\uparrow} = 13$, and
- $pf_{\mathrm{SHO}}^{\downarrow} = 3$.

It is clear that coverage is the the most important quality aspect from the network point of view (penalty factor pf_{COV}). Moreover, it imposes the biggest constraint to the optimization process, since the balance between SHO areas should not sacrifice network coverage. Another important characteristic that emerges from these values is the preference for minimizing areas where SHO capability is available in the uplink, but not in the downlink (penalty factor $pf_{\mathrm{SHO}}^{\uparrow}$). As it has been described in Section I, one of the consequences of such SHO arrangement produces serious interference rise in neighboring cells because of traffic increase in the serving cell (Figure 1), which may also result in service inaccessibility. The last factor $pf_{\mathrm{SHO}}^{\downarrow}$ imposes a penalty value over areas where SHO capability is available in the downlink, but not in the uplink. Remember that when accessing HSPA services, SHO is available only in the uplink. For this reason, the link throughput may benefit from SHO in the uplink if it is available. The relative lower importance of the last penalty factor compared with the other ones is directly related to the consequences of such unbalancing of SHO areas may have on

the network. In this case only HSPA throughput is affected, while the service accessibility should not be an issue, given there is enough uplink coverage [10].

C. Algorithm parameters

In this section we enumerate the parameters and their values used during the optimization process. In all three cases we have followed the naming conventions as they appear in the original publications [11], [12], [19].

1) DE: The parameters controlling the behavior of the DE algorithm have been set as follows:

- $NP = 100$, the population size;
- $G_{max} = 1000$, the maximum number of generations for the algorithm to run;
- $CR = 0.8$, the crossover constant; and
- $F = 0.5$, the mutation scaling factor.

2) DASA: As for DASA, we have set the parameters to the following values:

- $m = 10$, the number of ants;
- $b = 10$, the discrete base;
- $q = 0.2$, the pheromone dispersion factor;
- $s_+ = 0.01$, the global scale-increasing factor;
- $s_- = 0.01$, the global scale-decreasing factor; and
- $e = 1.0^{-2}$, the maximum parameter precision.

3) SA: There are only two parameters controlling SA, the initial temperature and the total number of iterations or evaluations:

- $t_{initial} = 125$,
- $it = 100,000$.

SA also allows to define the way the temperature is lowered during the annealing process. In this case, we have used the exponential-lowering schema.

D. Experimental environment

All experiments were carried out on a 4-core Intel i7 2.67 GHz desktop computer with 6 GB of RAM running a 64-bit Linux operating system. The implementation languages used were C and Python, with the latter mostly used as 'glue' to hold the different implementation parts together, as well as for I/O operations. To lower the time needed to run one optimization round, we have implemented the entire objective function evaluation using OpenCL and executed it on a nVidia GeForce GTX 260. This individual improvement exhibited more than 15x execution time speed-up when compared to the original CPU-only version.

VI. Results

A. Algorithm performance

In this section we examine the performance of the three selected algorithms in terms of solution quality and convergence speed. All experimental results were obtained after 30 independent runs, each of them limited to a maximum of 100,000 evaluations. The gathered results are shown in Table III.

Table III
Algorithm performance after 30 runs.

	Best	Worst	Mean	Std. deviation
DE	2,286,292.00	2,286,539.00	2,286,520.65	4.82
DASA	2,286,446.00	2,286,612.00	2,286,585.22	6.04
SA	2,293,350.00	2,295,570.00	2,294,626.50	159.61

As we may observe, DE reach the lowest objective function value, closely followed by DASA. Likewise, both algorithms reach very similar results for the worst, mean and standard deviation values. SA, on the other hand, did not achieve similar values, since its results are behind those of DE and DASA. Notice that even the best SA solution is no better than the worst solution of DASA. Moreover, the standard deviation exhibited by SA is many times bigger to those of DASA and DE, inducing the greater level of variance of its results.

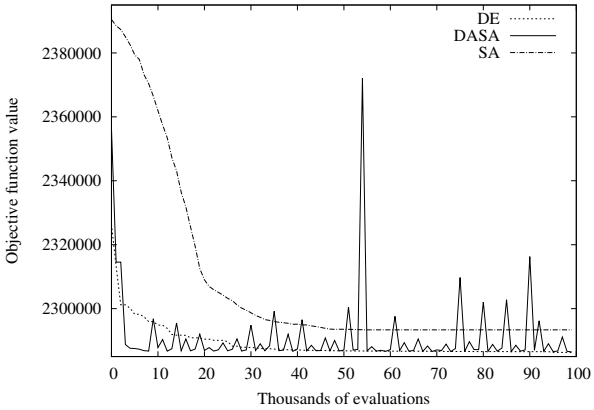

Figure 2. Algorithm convergence for the best obtained results.

The convergence of the best-recorded run of each of the three algorithms is shown in Figure 2. It is worth mentioning that every optimization run starts from a different solution, randomly constructed by picking a CPICH power setting, p_i^k, from every $P_i = \{p_i^1, p_i^2, ..., p_i^K\}$, $1 \leq k \leq |P_i|$, $\forall i \in N$. Notice how fast DASA converges to a good solution. After a number of evaluations without improvement, DASA resets itself and continues searching from a new random point within the search space [12], hence the displayed profile on the graph. Similarly, DE converges considerably fast, although not as fast as DASA does. It this case, DE does not reset itself if the current solution cannot be improved. Despite this, and based on the flat profile the graph exhibits towards the end of the optimization run, we are confident that 100,000 evaluations is an adequate stopping criterion for this algorithm. The last algorithm, SA, slowly converges towards the best solution found, even though it is not as good as the solutions found by DE and DASA.

The three convergence profiles shown in Figure 2 give a clearer notion about the way these algorithms explore the search space of the balancing problem.

Table IV
OPTIMIZATION RESULTS.

	Uncovered area	Covered area, no SHO	Normal SHO area	no SHO$^{\downarrow}$, SHO$^{\uparrow}$	SHO$^{\downarrow}$, no SHO$^{\uparrow}$	Total
Before optimization	63.00 %	15.11 %	15.73 %	1.80 %	4.36 %	100.00 %
DE solution	60.23 %	16.13 %	16.09 %	1.47 %	6.08 %	100.00 %
DASA solution	60.24 %	16.16 %	16.90 %	1.46 %	5.24 %	100.00 %
SA solution	60.42 %	16.55 %	15.97 %	1.56 %	5.50 %	100.00 %
DE improvement	+4.40 %	+6.75 %	+2.29 %	+18.33 %	-39.45 %	—
DASA improvement	+4.38 %	+6.95 %	+7.44 %	+18.88 %	-20.18 %	—
SA improvement	+4.09 %	+9.53 %	+1.52 %	+13.33 %	-26.15 %	—
Avg. improvement	+4.29 %	+7.74 %	+3.75 %	+16.85 %	-28.59 %	—

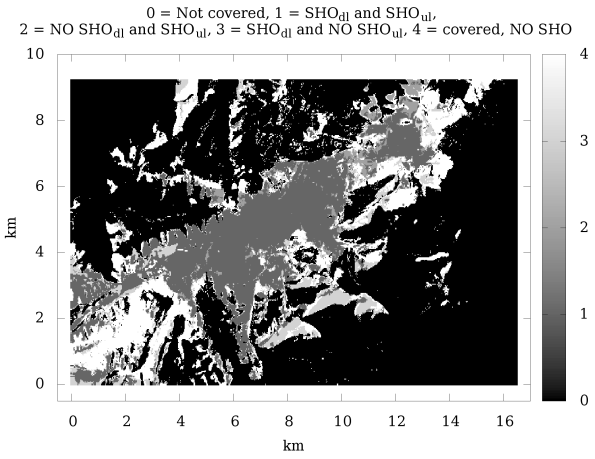

Figure 3. Spatial distribution of SHO areas, before optimization.

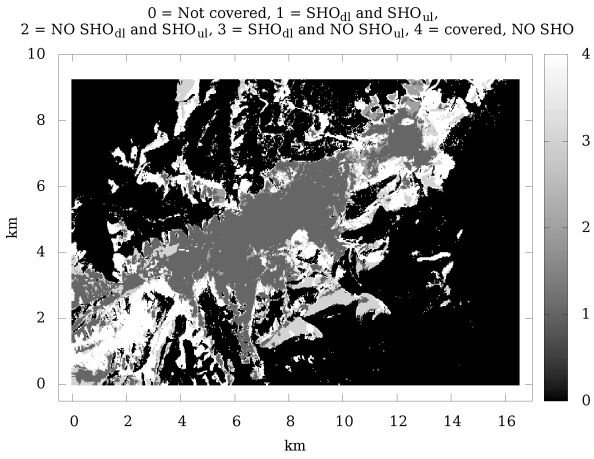

Figure 4. Spatial distribution of SHO areas, after optimization.

B. Interpretation

Table IV presents the analysis of the obtained results from the network point of view. After 30 independent runs of each of the three algorithms, the best results obtained where evaluated for improvement and decline of each of the measured network aspects. The results are shown in Table IV, where '+' indicates improvement and '-' indicates decline of a given criteria. We may observe that the measured criteria have been significantly improved. The only exception is the measure labeled as 'SHO$^{\downarrow}$, no SHO$^{\uparrow}$', which shows an expected change, since it is the optimization aspect with the lowest penalty factor value.

Coverage has been improved with an average of 4.29%, whereas the coverage area where there is no SHO capability has been increased 7.74% in average. The SHO areas, where this facility is available in both the downlink and uplink, has also been improved 3.75% in average. This particular improvement is interesting from the optimization point of view, because it had no explicit penalty factor set. Therefore we understand this enhancement as a consequence of the completeness of criteria, taking into account in the objective function.

The second most important optimized aspect in the balancing problem is the proportion of areas with uplink SHO and no SHO in the downlink (labeled as 'no SHO$^{\downarrow}$, SHO$^{\uparrow}$' in Table IV). This particular condition has been improved by almost 17% in average, greatly reducing the possibility of interference in neighboring cells when serving HSPA traffic. The last measured aspect takes into account areas with downlink SHO and no SHO in the uplink (labeled as 'SHO$^{\downarrow}$, no SHO$^{\uparrow}$' in Table IV). This condition, although it hasn't improved, does not expose the mobile network to malfunctioning, only to reduced throughput within these specific areas. However, the reduced throughput is relative, since there are many cells capable of serving HSDPA data access, as the downlink SHO condition confirms. For this reason, the serving cell should not only deliver HSDPA, but should also take care of the user signaling and power control, received in the uplink. Obviously, this is feasible only where uplink coverage is guaranteed.

It is worth mentioning that these results were obtained for a working mobile network with live data. Moreover, the hard constraints imposed to the optimization process (CPICH power limited within the ± 2 dB interval) ensure that the resulting configuration may be immediately applied to the mobile network. This fact can be contrasted with the spatial distribution of each of the optimized aspects, before and after applying the optimization results, as it is shown in Figures 3 and 4.

The lack of any prominent visual change in Figures 3 and 4 is a desired consequence of the fine-tuning procedure the network has been exposed to. Still, the improvements are present precisely over the areas that are most exposed to malfunctioning due to unbalanced SHO, e.g. their borders.

VII. Conclusion

We have presented the problem of balancing SHO areas in UMTS networks and characterized some of the consequences unbalanced SHO areas have on the quality of HSPA services. By using a static network simulator, based on a state-of-the-art mathematical model, we have located downlink and uplink SHO areas. Both the mathematical model and the penalty scores of the objective function have been set according to the configuration and layout of a real mobile network, deployed in Slovenia by Telekom Slovenije, d.d.. The balancing problem has been tackled by three optimization algorithms, namely DE, DASA and SA. To the best of our knowledge, there is no reference in the literature to a simulation-based approach to find active SHO areas in the downlink and uplink. Additionally, as far as we know, the SHO balancing problem, as described in this paper, has not yet been tackled by any formal optimization method.

All three algorithms were able to improve the given network configuration, being DE the most successful one. The presented results confirm that a great proportion of the non-aligned SHO areas, that were present before the optimization, were corrected, therefore significantly reducing the possibility of HSPA-service inaccessibility within these areas. Additionally, network coverage has been improved, while all other essential network services were not altered.

One of the key advantages of the presented method is that it targets the optimization of a deployed network, for which the focus is put on fine-tuning an existing configuration instead of creating complete new solutions. Furthermore, a deployed network has a great number of hard-constraints that should be taken into account at the optimization stage, yet our approach is simple and versatile enough for it to be used in practically any working UMTS network. Moreover, our model is applicable for mobile networks in heterogeneous environments, because it imposes no restrictions regarding cell layout or radio propagation characteristics.

To further improve the presented results, fast power control should be included in the simulations, since it is a valuable element of a WCDMA mobile system. Another extension of the current work is to incorporate antenna tilt as an additional objective of the optimization process. This should certainly include experimentation with models and algorithms that support multiobjective optimization.

Acknowledgment

The authors would like to especially thank the radio engineers at Telekom Slovenije, d.d., for cooperating and sharing their professional expertise throughout the creation of this work. This project was co-financed by the European Union, through the European Social Fund.

References

[1] L. Chen, K. Sandrasegaran, R. Basukala, F.M. Madani, and C.C. Lin. Impact of soft handover and pilot pollution on video telephony in a commercial network. In *Communications (APCC), 2010 16th Asia-Pacific Conference on*, pages 481–486. IEEE, 2010.

[2] L. Chen and D. Yuan. CPICH Power Planning for Optimizing HSDPA and R99 SHO Performance: Mathematical Modelling and Solution Approach. In *Proc. IFIP 1st Wireless Days Conference (WD)*, pages 1–5, 2008.

[3] L. Chen and D. Yuan. Coverage planning for optimizing HSDPA performance and controlling R99 soft handover. *Telecommunication Systems*, pages 1–12, 2011.

[4] S. Das and P.N. Suganthan. Differential evolution: A survey of the state-of-the-art. *Evolutionary Computation, IEEE Transactions on*, (99):1–28, 2010.

[5] M. Dorigo, M. Birattari, and T. Stutzle. Ant colony optimization. *Computational Intelligence Magazine, IEEE*, 1(4):28–39, 2006.

[6] A. Eisenblätter, A. Füngenshuch, H. F. Geerdes, D. Junglas, T. Koch, and A. Martin. Optimization methods for UMTS radio network planning. In *Intl. Conference on Operations Research*, pages 31–38. Springer, September 2003.

[7] M. Garcia-Lozano, S. Ruiz, and J. Olmos. CPICH power optimisation by means of simulated annealing in an UTRA-FDD environment. *Electronics Letters*, 39(23):1676–7, 2003.

[8] S.C. Ghosh, R.M. Whitaker, S.M. Allen, and S. Hurley. Optimising CDMA Cell Planning with Soft Handover. *Wireless Personal Communications*, pages 1–27, 2011.

[9] H. Holma and A. Toskala. *WCDMA for UMTS: Radio access for third generation mobile communications, Third Edition*. John Wiley & Sons, Inc. New York, NY, USA, 2005.

[10] H. Holma and A. Toskala. *HSDPA/HSUPA For UMTS*. John Wiley & Sons, 2006.

[11] S. Kirkpatrick, C.D. Gelatt, and M.P. Vecchi. Optimization by simulated annealing. *Science*, 220(4598):671, 1983.

[12] P. Korošec, J. Šilc, and B. Filipič. The differential ant-stigmergy algorithm. *Information Sciences*, 2010.

[13] J. Laiho, A. Wacker, and T. Novosad. *Radio Network Planning and Optimisation for UMTS*. John Wiley & Sons, Inc. New York, NY, USA, 2002.

[14] J. Lempiäinen and M. Manninen. *UMTS Radio Network Planning, Optimization and QoS Management for Practical Engineering Tasks*. Kluwer Academic Publishers Norwell, MA, USA, 2004.

[15] M. Nawrocki, H. Aghvami, and M. Dohler. *Understanding UMTS radio network modelling, planning and automated optimisation: theory and practice*. John Wiley & Sons, 2006.

[16] K.V. Price, R.M. Storn, and J.A. Lampinen. *Differential evolution: a practical approach to global optimization*. Springer-Verlag New York Inc., 2005.

[17] I. Siomina. Pilot power management in WCDMA networks: coverage control with respect to traffic distribution. In *Proceedings of the 7th ACM international symposium on Modeling, analysis and simulation of wireless and mobile systems*, pages 276–282. ACM New York, NY, USA, 2004.

[18] I. Siomina and D. Yuan. Minimum pilot power for service coverage in WCDMA networks. *Wireless Networks*, 14(3):393–402, 2008.

[19] R. Storn and K. Price. Differential evolution–a simple and efficient heuristic for global optimization over continuous spaces. *Journal of global optimization*, 11(4):341–359, 1997.

[20] B. Suman and P. Kumar. A survey of simulated annealing as a tool for single and multiobjective optimization. *Journal of the operational research society*, 57(10):1143–1160, 2005.

[21] TEMS CellPlanner. http://www.ericsson.com/tems/.

[22] Third Generation Partnership Project. *Technical specification group services and systems aspects: Network architecture v3.6.0 (Release 1999)*. http://www.3gpp.org/.

[23] S. Ying, F. Gunnarsson, K. Hiltunen, E. Res, and C. Beijing. CPICH power settings in irregular WCDMA macro cellular networks. *14th IEEE Proceedings on Personal, Indoor and Mobile Radio Communications, 2003. PIMRC 2003*, 2, 2003.